

Igor Travěnek • Ladislav Šamaj

Low-temperature anomalies in one-dimensional exactly solvable fluids

Received: / Accepted:

Abstract Previous experiments and numerical simulations have revealed that a limited number of two- and three-dimensional particle systems contract in volume upon heating isobarically. This anomalous phenomenon is known as negative thermal expansion (NTE). The present paper focuses on the possibility of NTE in exactly solvable one-dimensional fluids. Firstly, the quantization of classical pure hard rods (free of NTE) does not induce NTE which indicates an unimportant role of quantum mechanics in the topic. Secondly, the classical hard rods with various types of soft nearest-neighbor interactions that contain a basin of attraction with only one minimum are investigated. The ground-state analysis reveals that, for certain potentials, increasing the pressure can lead to a discontinuous jump in the mean spacing between particles. The low-temperature analysis of the exact equation of state indicates that the NTE anomaly is present if the curvature of the soft potential increases with the distance between particles or if the potential exhibits a singularity within the basin of attraction. Isotherms of the compressibility factor, which measures the deviation of the thermodynamic behavior of a real gas from that of an ideal gas, demonstrate typical plateau or double-plateau shapes in large intervals of particle density.

Keywords one-dimensional fluids; classical and quantum hard rods; nearest-neighbor interactions; equation of state; exact thermodynamics; negative thermal expansion.

1 Introduction

Standard solid and fluid materials expand in volume when heated under constant pressure. However, there are special materials that contract in volume

Institute of Physics, Slovak Academy of Sciences, Dúbravská cesta 9, SK-84511 Bratislava, Slovakia
E-mail: Igor.Travenec@savba.sk and Ladislav.Samaj@savba.sk

upon heating; this anomalous phenomenon is known as negative thermal expansion (NTE).

NTE has been experimentally observed in three-dimensional (3D) substances with anisotropic intermolecular pairwise interactions. One well-known example is ice under atmospheric pressure which exhibits NTE at low temperatures $\lesssim 63K$ [1, 2] as well as upon melting ice into liquid water in the temperature interval $0 - 3.98 \text{ }^\circ C$ [3, 4]. NTE has also been detected in graphene [5] and complex compounds like zirconium tungstate ZrW_2O_8 [6], diamond and zinc-blende semiconductors [7], $Lu_2W_3O_{12}$ [8], etc.

NTE has been observed in computer simulations of two-dimensional (2D) and 3D single-component classical (i.e., non-quantum) systems with *isotropic* pair interactions [9] provided that the soft-core potential $\varphi(r)$ has a region of attraction with increasing curvature. In one dimension (1D), the necessary and sufficient condition for NTE as stated by Kuzkin [10] is

$$\varphi'''(l) > 0, \quad (1.1)$$

where l is the mean spacing between particles at a given temperature.

Other models of identical particles with *repulsive* isotropic interactions that exhibit NTE also exist. NTE arises at low temperatures in 2D systems with a specific topography of the energy landscape [11, 12]. The NTE anomaly was detected using computer simulations in 3D repulsive potentials with two competing length scales: the hard-core diameter a and a finite soft-core range $a' > a$, see references [13–23]. The repulsive soft-core potentials used in simulations were mainly the square shoulder potential [24, 25] and the linear ramp potential of Jagla [26], or smoothed potentials [13, 19, 20, 27, 28]. It is generally believed that repulsive potentials with two length scales always exhibit water-like anomalies [20, 27].

NTE occurs in the 3D Gaussian core model with an interaction potential that is analytic everywhere [29].

In one dimension (1D), there is a large family of classical fluids consisting of particles that interact pairwise through a potential which are exactly solvable in thermal equilibrium at temperature T .

The simplest 1D system of this type is the Tonks gas of hard rods with the interaction potential

$$\phi(x) = \begin{cases} \infty & \text{if } |x| < a, \\ 0 & \text{if } |x| \geq a, \end{cases} \quad (1.2)$$

where a represents the diameter of the hard core around each particle. For the classical version of this model, Tonks [30] derived the equation of state (EoS) which relates the particle density to temperature T and pressure $p \geq 0$. This simple model is free of NTE anomaly. The two-body distribution function of classical hard rods was calculated earlier [31]. The quantum version of 1D hard rods was solved exactly by using the Bethe ansatz in reference [32], see also textbook [33].

Takahashi [34] solved a more general classical model with interactions only among nearest neighbors using the canonical ensemble. Bishop and Boonstra [35] performed a rederivation of the EoS for the Takahashi gas within the

isothermal-isobaric ensemble. The many-particle distribution functions have been derived in reference [36].

Interactions among all particles were reduced in the Takahashi gas to the nearest-neighbor pairs approximately ad-hoc “by hand”. Let us now consider 1D hard rods of diameter a interacting via the two-length-scales pair potential

$$\phi(x) = \begin{cases} \infty & \text{if } |x| < a, \\ \varphi(x) & \text{if } a \leq |x| < a', \\ 0 & \text{if } |x| \geq a', \end{cases} \quad (1.3)$$

where $\varphi(x) = \varphi(-x)$ and the range a' of the soft-core potential $\varphi(x)$ is restricted by $a' \leq 2a$. For a given particle, this restriction implies that hard cores of first neighbors prevent interaction with second neighbors, effectively reducing of the interaction potential to nearest neighbors only without any ad-hoc assumptions. The exact solution of thermal equilibrium of 1D fluids with nearest-neighbor interactions (1.3) includes systems of identical particles together with mixtures [37–41], see books [42, 43]. A scaling regime in which the system exhibits a second-order phase transition was proposed by Jones [44].

Recently[45], exactly solvable 1D fluids of hard rods with various types of soft *purely repulsive* nearest-neighbor interaction potentials $\varphi(x) > 0$, such as the square shoulder, linear and quadratic ramps and certain logarithmic potentials were examined for the NTE phenomenon in the low-temperature region. These particle systems were found to exhibit NTE anomalies, with the presence of the anomaly depending greatly on the shape of the core-softened potential. In some cases, NTE was associated with equidistant ground states jumps in chain spacing $a' \rightarrow a$ at specific pressures. Kuzkin’s necessary and sufficient condition for NTE (1.1) did not apply to these systems. Isotherms of the compressibility factor, which measures the deviation of the thermodynamic behavior of a real gas from an ideal gas, were shown to display both monotonous and non-monotonous behaviors as functions of the particle density, with a paradoxical weakening of pressure as density increases.

The present paper continues in focusing on the possibility of NTE in exactly solvable 1D fluids. Firstly, we study the classical and quantum versions of pure hard rods and show that the inclusion of quantum fluctuations in classical model (which itself is free of NTE) does not induce NTE. This indicates an unimportant role of quantum mechanics in the topic. Secondly, classical hard rods with soft nearest-neighbor interaction potentials that contain a basin of attraction with only one minimum (except for the square well potential) are considered. Some of the soft potentials are depicted in figure 1. The ground-state and low-temperature analysis of EoS indicates that NTE anomaly is present if the curvature of the interaction potential increases with the distance between particles, in agreement with Kuzkin’s condition (1.1). Another possible cause for NTE is a singularity of the potential within the basin of attraction. Isotherms of the compressibility factor show to exhibit plateau or double-plateau shapes in large intervals of particle density.

The paper is organized as follows. Section 2 discusses the general formalism for exactly solvable 1D fluids with nearest-neighbor interactions of the type (1.3) with $a' \leq 2a$, in the ground state at $T = 0$ or at arbitrary T .

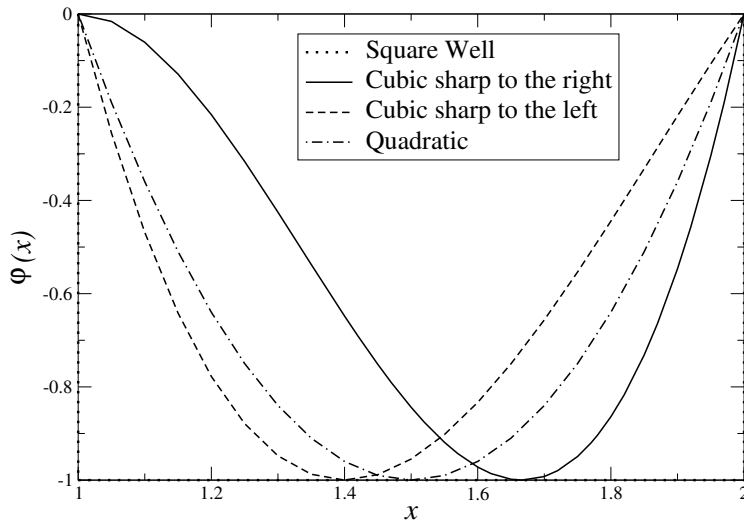


Fig. 1 Some of the interaction potentials considered in this work: the square well potential and polynomial models. The length scale with the hard-core diameter $a = 1$ is used.

The compressibility factor is introduced. The derivation and analysis of EoS for the classical and quantum versions of Tonks model (1.2) are presented in section 3. The square well model with a constant negative potential between a and a' is studied in section 4. The polynomial (quadratic and cubic) models are analyzed in section 5. Section 6 deals with interaction potentials that exhibit a singularity inside the basin of attraction, specifically at, to the left and to the right of the minimum point. Section 7 provides a brief recapitulation and concluding remarks.

2 General formalism for 1D classical fluids

2.1 Exact formulas for the EoS

N identical particles of the 1D classical fluid move in a continuous box of length L , say with periodic boundary conditions. The thermodynamic limit $L \rightarrow \infty$ and $N \rightarrow \infty$, while keeping the particle number density $n = N/L$ fixed, is considered. The pair potential $\phi(x)$ is of the form (1.3) with the restriction $a' \leq 2a$, ensuring that each particle interacts only with its nearest neighbors. The hard-core condition $\phi(x) = \infty$ for $|x| \in [0, a]$ fixes the order of the particles on the line.

The soft-core potential $\varphi(x)$ is supposed to be attractive,

$$\varphi(x) \leq 0, \quad x \in [a, a'], \quad (2.1)$$

with just one minimum at point $x = a_m$ ($a < a_m < a'$) at which its derivative with respect to x vanishes:

$$\left. \frac{\partial \varphi(x)}{\partial x} \right|_{x=a_m} = 0. \quad (2.2)$$

The only exception from this condition is the square well potential (section 4) possessing an infinitely degenerate minimum. The derivative is assumed to be negative for $x \in (a, a_m)$ and positive for $x \in (a_m, a')$:

$$\frac{\partial \varphi(x)}{\partial x} < 0 \quad \text{for } x \in (a, a_m), \quad \frac{\partial \varphi(x)}{\partial x} > 0 \quad \text{for } x \in (a_m, a'). \quad (2.3)$$

Moreover, the potential is assumed to be continuous at the interaction border $x = a'$,

$$\varphi(a') = 0. \quad (2.4)$$

Without any loss of generality, in numerical evaluations of exact formulas the soft-core potential is taken to vanish also in the hard-core limit as $x \rightarrow a^+$,

$$\varphi(x \rightarrow a^+) = 0. \quad (2.5)$$

The value of the potential at the minimum point $\varphi(a_m)$ will usually be fixed to -1 .

Particles are in thermal equilibrium with the thermostat at temperature T , or inverse temperature $\beta = 1/(k_B T)$ where the Boltzmann constant k_B will be set to unity. The model is exactly solvable in the isothermal-isobaric ensemble, see reference [43] for the notation. Instead of the particle density n , EoS will be formulated in terms of the averaged distance between particle (reciprocal density) $l = 1/n$. The exact EoS can be expressed in terms of the Laplace transform of the pair Boltzmann factor $e^{-\beta\phi(x)}$,

$$\widehat{\Omega}(s) = \int_0^\infty dx e^{-xs} e^{-\beta\phi(x)} \quad (2.6)$$

and of its derivative

$$\widehat{\Omega}'(s) \equiv \frac{\partial \widehat{\Omega}(s)}{\partial s} = - \int_0^\infty dx x e^{-xs} e^{-\beta\phi(x)} \quad (2.7)$$

as follows:

$$l(\beta, p) = - \frac{\widehat{\Omega}'(\beta p)}{\widehat{\Omega}(\beta p)} = \frac{\int_0^\infty dx x e^{-\beta p x} e^{-\beta\phi(x)}}{\int_0^\infty dx e^{-\beta p x} e^{-\beta\phi(x)}}. \quad (2.8)$$

For the two-length-scales pair potential (1.3), this formula can be written as

$$l(\beta, p) = - \frac{1}{\beta} \frac{\partial}{\partial p} \ln \left[\int_a^{a'} dx e^{-\beta f(x)} + \frac{e^{-\beta p a'}}{\beta p} \right], \quad (2.9)$$

where

$$f(x) \equiv \varphi(x) + px \quad (2.10)$$

and $p > 0$; the dependence of $f(x)$ on p will not be explicitly expressed to save space.

The integral in the exact formula for the mean spacing (2.9) can be expressed in terms of elementary or special functions for certain forms of the soft-core potential $\varphi(x)$. In that case the ground-state and low- T (large- β) analyses can be easily done explicitly. In the opposite case, the ground-state analysis and a systematic low- T expansion can be done for general $\varphi(x)$ by using a procedure outlined below.

2.2 Ground state and the leading low- T correction

In general, it is a difficult task to prove that the ground state of interacting classical particles is periodic [46–48]. The situation is simpler in 1D fluids where a number of theorems have been proven for various kinds of interaction potentials [49–51]. For the considered hard-core potential with a finite-range soft potential (1.3), Radin and Schulman proved the periodicity of the 1D ground state in reference [52].

The ground-state formula for the mean spacing l and its low- T (large- β) corrections can be systematically generated from the formula (2.9) by using the standard saddle-point method applied to the function $f(x)$ in the integral under the logarithm. Let the function $f(x)$ have its minimum at x^* , i.e.,

$$\left. \frac{\partial f(x)}{\partial x} \right|_{x=x^*} = 0, \quad \left. \frac{\partial^2 f(x)}{\partial x^2} \right|_{x=x^*} > 0. \quad (2.11)$$

In view of definition (2.10), this condition is equivalent to the one

$$p = - \left. \frac{\partial \varphi(x)}{\partial x} \right|_{x=x^*}. \quad (2.12)$$

The inversion of this relation defines the ground-state function $x^*(p)$. Inserting the leading term of the Taylor expansion

$$f(x) = f(x^*) + O\left((x - x^*)^2\right) \quad (2.13)$$

into the integral in (2.9), one gets

$$l(\beta, p) \approx \frac{\partial}{\partial p} f(x^*(p)) - \frac{1}{\beta} \frac{\partial}{\partial p} \ln \left\{ (a' - a) + \frac{1}{\beta p} e^{-\beta[p(a' - x^*) - \varphi(x^*)]} \right\}. \quad (2.14)$$

The second term on the rhs of this equation is exponentially small, specifically of type $\exp(-c\beta)$ with $c > 0$, and therefore can be neglected in the limit $\beta \rightarrow \infty$. The first term on the rhs of (2.14) can be written as

$$\begin{aligned} \frac{\partial}{\partial p} f(x^*(p)) &= \frac{\partial}{\partial p} [\varphi(x^*(p)) + px^*(p)] \\ &= \frac{\partial \varphi(x^*)}{\partial x^*} \frac{\partial x^*}{\partial p} + x^*(p) + p \frac{\partial x^*}{\partial p} \\ &= x^*(p), \end{aligned} \quad (2.15)$$

where the transition from the second to the third line follows from (2.12). It is clear that $x^*(p)$ determined by equation (2.12) is nothing but the ground-state spacing,

$$l(T = 0, p) = x^*(p). \quad (2.16)$$

In the limit $p \rightarrow 0^+$, x^* coincides with the minimum point of the potential $\varphi(x)$,

$$\lim_{p \rightarrow 0^+} l(T = 0, p) = a_m. \quad (2.17)$$

On the other hand, $x^*(p)$ attains its hard-core minimum equal to a at the ‘‘incompressibility’’ pressure p_i given by

$$p_i = - \left. \frac{\partial \varphi(x)}{\partial x} \right|_{x=a}. \quad (2.18)$$

Due to the presence of the hard core, the ground-state spacing remains to be equal to a also for all pressures larger than p_i ,

$$l(T = 0, p) = a \quad \text{for all } p \geq p_i. \quad (2.19)$$

To obtain the leading low- T correction to the ground-state formula (2.16) one must consider the next term of the Taylor expansion of $f(x)$ around the point x^* ,

$$f(x) = f(x^*) + \frac{1}{2!} \varphi''(x^*) (x - x^*)^2 + O\left((x - x^*)^3\right), \quad (2.20)$$

where the equality $f''(x) = \varphi''(x)$ was utilized. Neglecting terms of order $(x - x^*)^3$ and substituting the above expansion into the integral in (2.9), one obtains:

$$l(\beta, p) \approx x^*(p) - \frac{1}{\beta} \frac{\partial}{\partial p} \ln \left\{ \int_a^{a'} dx e^{-\frac{\beta}{2} \varphi''(x^*) (x - x^*)^2} + \frac{1}{\beta p} e^{-\beta [p(a' - x^*) - \varphi(x^*)]} \right\}. \quad (2.21)$$

By using the substitution $y = \sqrt{\beta \varphi''(x^*)/2} (x - x^*)$, the integral in the second term on the rhs of (2.21) can be transformed to

$$\sqrt{\frac{2}{\beta \varphi''(x^*(p))}} \int_{\sqrt{\beta \varphi''(x^*)/2} (a - x^*)}^{\sqrt{\beta \varphi''(x^*)/2} (a' - x^*)} dy e^{-y^2}. \quad (2.22)$$

In view of the inequalities $(a' - x^*) > 0$ and $(a - x^*) < 0$, in the considered $\beta \rightarrow \infty$ limit the lower and upper bounds of integration can be substituted by $-\infty$ and ∞ , respectively. Since $p(a' - x^*) - \varphi(x^*) > 0$ for the attractive soft-core potential $\varphi(x) \leq 0$, the integral is dominant with respect to the exponentially small term under the logarithm in equation (2.21), resulting in the low- T expansion:

$$l(T, p) = x^*(p) + \frac{T}{2} \frac{\partial}{\partial p} \ln \left(\left. \frac{\partial^2 \varphi(x)}{\partial x^2} \right|_{x=x^*(p)} \right) + o(T). \quad (2.23)$$

The validity of the analysis above is limited to pressures $0 \leq p < p_i$. The reason is that for $p \geq p_i$ the coordinate $x = a$ no longer yields the minimum of $f(x) \equiv \varphi(x) + px$. Therefore, the Taylor expansion of $f(x)$ around the point $x = a$ also includes the linear term:

$$f(x) = f(a) + (p - p_i)(x - a) + \frac{1}{2}\varphi''(a)(x - a)^2 + \dots; \quad (2.24)$$

here, we have utilized the definition of p_i (2.18) and the evident equality $f''(x) = \varphi''(x)$. By substituting the Taylor expansion (2.24) into the integral in (2.9) and employing the substitution $y = x - a$, we obtain

$$l(\beta, p) \approx a - \frac{1}{\beta} \frac{\partial}{\partial p} \ln \left\{ \int_0^{a'-a} dy e^{-\beta(p-p_i)y - \frac{\beta}{2}\varphi''(a)y^2} + \frac{1}{\beta p} e^{-\beta[p(a'-a) - \varphi(a)]} \right\}. \quad (2.25)$$

Since $p(a' - a) - \varphi(a) > 0$, the exponentially small term can be neglected with respect to the integral in the limit $\beta \rightarrow \infty$ and one arrives at

$$l(\beta, p) \approx a + \frac{\int_0^{a'-a} dy y e^{-\beta(p-p_i)y - \frac{\beta}{2}\varphi''(a)y^2}}{\int_0^{a'-a} dy e^{-\beta(p-p_i)y - \frac{\beta}{2}\varphi''(a)y^2}}. \quad (2.26)$$

- For $p = p_i$, the term linear in y disappears and one finds in the $\beta \rightarrow \infty$ limit that

$$l(T, p_i) = a + \sqrt{\frac{2}{\pi\varphi''(a)}}\sqrt{T} + o(\sqrt{T}). \quad (2.27)$$

Note the transition from the analytic expansion in T for $0 \leq p < p_i$ (2.23) to a singular expansion in \sqrt{T} at $p = p_i$.

- When $p > p_i$, the terms linear in y dominate over the quadratic ones and one gets

$$l(T, p) = a + \frac{1}{p - p_i}T + o(T), \quad p > p_i. \quad (2.28)$$

The prefactor to T diverges as p goes to p_i from above which is a sign of the change in the analytic form of the leading low- T correction from T for $p > p_i$ to \sqrt{T} at $p = p_i$. Notice that an infinite pressure has to be applied to squeeze the particles to their smallest hard-core distance a if $T > 0$, in contrast to the $T = 0$ ground state with $l(0, p) = a$ for all $p \geq p_i$.

The scenario above holds if $x^*(p)$ changes continuously from a_m at $p \rightarrow 0$ to a at $p = p_i$. Possible exceptions associated with a discontinuity of $x^*(p)$ will be discussed in particular cases in section 5.

2.3 The compressibility factor

The deviation of thermodynamic behavior of real gases from the EoS of an ideal gas $\beta p = n$ is measured by the compressibility factor Z defined as:

$$Z(\beta, n) \equiv \frac{\beta p}{n}. \quad (2.29)$$

In the low-density limit as $n \rightarrow 0$, it holds that

$$Z(\beta, n) \underset{n \rightarrow 0}{\sim} 1. \quad (2.30)$$

Another regime that can be treated rigorously is the neighborhood of the close packed limit $l \rightarrow a^+$ (or $na \rightarrow 1^-$) when $\beta p \rightarrow \infty$ [45]. In particular,

$$Z(\beta, n) = \frac{1}{1 - an} - \beta \varphi'(a)a - \beta [\varphi'(a)a + 2\varphi''(a)a^2] (1 - an) + O[(1 - an)^2]. \quad (2.31)$$

The leading singular term of this expansion is universal, i.e., independent of the model's parameters, except for the hard core diameter a . The only known exception from this singular behavior is the sticky balls model [42, 43] with the leading term of the form $Z \propto 1/\sqrt{1 - an}$.

3 1D Tonks gas

3.1 Classical hard rods

For the classical 1D fluid of hard rods with the interaction potential (1.2), the Laplace transform of the pair Boltzmann factor (2.6) reads as

$$\widehat{\Omega}(s) = \frac{e^{-as}}{s}. \quad (3.1)$$

By applying (2.8), the EoS for the reciprocal density takes the form

$$l(T, p) = a + \frac{T}{p}. \quad (3.2)$$

When a approaches zero (pointlike particles), the EoS of the ideal gas $\beta p = n$ is obtained.

In the low-temperature limit $T \rightarrow 0$ and for any positive pressure $p > 0$, the particle spacing $l(0, p)$ becomes the lattice constant a of the close packed array of hard rods in the ground state. As temperature T increases, the average distance between particles grows linearly with T and diverges in the high-temperature limit $T \rightarrow \infty$. This behavior is due to thermal fluctuations which weaken energy bounds among particles. NTE anomaly is absent for classical 1D Tonks gas.

The compressibility factor is given by

$$Z = \frac{\beta p}{n} = \frac{1}{1 - an}. \quad (3.3)$$

It involves only the leading term of the expansion (2.31).

3.2 Quantum hard rods

The exact solution of 1D quantum hard rods [32] was given as the simplest example of general formalism of analytic and thermodynamic Bethe ansatz in worked-out exercises of textbook [33]. Hard rods are taken as identical spinless particles of mass m , it does not matter whether bosons or fermions (the relationship between the particle spin and Fermi/Bose statistics is purposely ignored in the field of integrable systems). In units of reduced Planck constant $\hbar = 1$ and $2m = 1$, the thermal de Broglie wavelength reads as

$$\lambda_B \equiv \hbar \sqrt{\frac{2\pi\beta}{m}} = 2\sqrt{\pi\beta}. \quad (3.4)$$

The analytic Bethe ansatz for 1D quantum hard rods is discussed in section 1.6 of [33].

The zero-temperature EoS

$$l(0, p) - a = \left(\frac{2\pi^2}{3p}\right)^{1/3} \quad (3.5)$$

is derived in exercise 2.4 of section 2 in textbook [33]. It is seen that the particle spacing in the quantum case depends on p . Its classical hard-core value $l(0, p) = a$ is obtained only in the limit $p \rightarrow \infty$ while $l(0, p)$ diverges as $p \rightarrow 0$. These properties of $l(0, p)$ are related to the uncertainty principle in quantum mechanics.

The finite-temperature EoS is derived within the grand canonical ensemble in exercise 3.3 of section 3 in textbook [33]. Introducing the shifted chemical potential $\tilde{\mu} \equiv \mu - ap$ and the rescaled particle density

$$\tilde{n} \equiv \frac{n}{1 - an} = \frac{1}{l - a}, \quad (3.6)$$

it holds that

$$p = \frac{1}{\pi} \int_{-\infty}^{\infty} dk \frac{k^2}{e^{\beta(k^2 - \tilde{\mu})} + 1} = -\frac{1}{2\sqrt{\pi}\beta^{3/2}} \text{Li}_{3/2}(-e^{\beta\tilde{\mu}}) \quad (3.7)$$

$$\tilde{n} = \frac{1}{2\pi} \int_{-\infty}^{\infty} dk \frac{1}{e^{\beta(k^2 - \tilde{\mu})} + 1} = -\frac{1}{2\sqrt{\pi}\beta^{1/2}} \text{Li}_{1/2}(-e^{\beta\tilde{\mu}}). \quad (3.8)$$

Here, the polylogarithm function $\text{Li}_n(z)$ is defined in the complex z -plane over the open unit disk as the series

$$\text{Li}_n(z) = \sum_{k=1}^{\infty} \frac{z^k}{k^n}. \quad (3.9)$$

The relation between the deviation of the particle spacing $l - a = 1/\tilde{n}$ and temperature $T = 1/\beta$ at fixed pressure p can be obtained via calculation of the parameter $\tilde{\mu}$ from relation (3.7) and its subsequent substitution into (3.8).

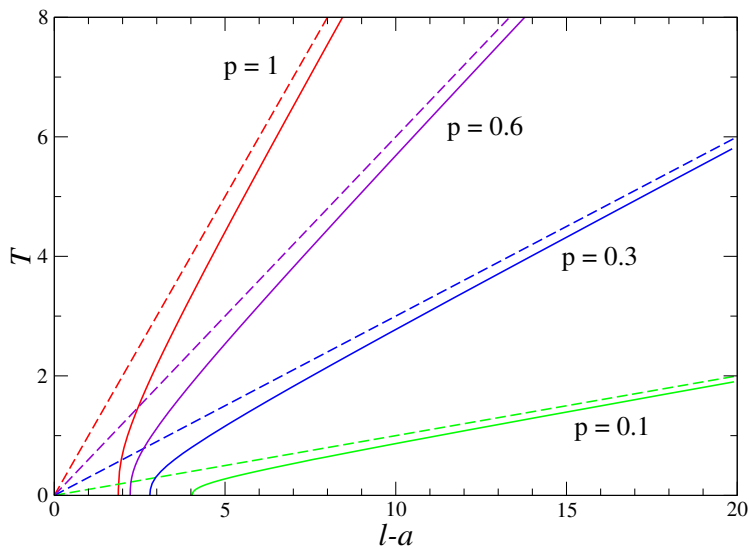


Fig. 2 1D system of pure hard rods. The plots of temperature T as the function of the shifted mean spacing $l - a$ for the pressures $p = 0.1, 0.3, 0.6$ and 1 . The solid/dashed curves correspond to the quantum/classical version of the model.

The high-temperature and low-temperature virial expansions of the pressure p are constructed in exercise 3.5 of section 3 in textbook [33]. At high temperatures one gets

$$\frac{\beta p}{\tilde{n}} = 1 + \frac{1}{2^{3/2}} (\lambda_B \tilde{n}) + \left(\frac{1}{2} - \frac{2}{3^{3/2}} \right) (\lambda_B \tilde{n})^2 + O(1/T^{3/2}). \quad (3.10)$$

Note that since $\lambda_B \rightarrow 0$ in the high-temperature limit $\beta \rightarrow 0$, the expansion (3.10) passes to the classical EoS (3.2) as it should be by the correspondence principle in quantum mechanics. At low temperatures one gets

$$p = \frac{2\pi^2}{3} \tilde{n}^3 + \frac{1}{6\tilde{n}} T^2 + \frac{1}{30\pi^2 \tilde{n}^5} T^4 + O(T^6). \quad (3.11)$$

In this paper, instead of presenting the plots of l versus T for fixed p we prefer to present the plots T versus l (or $l - a$) for fixed p because the NTE phenomenon is better seen in this format. The plots of T versus $l - a$ for the pressures $p = 0.1, 0.3, 0.6$ and 1 are pictured in figure 2 by the solid/dashed curves for the quantum/classical version of the model. Quantum curves are approaching classical ones at higher temperatures quite slowly; as follows from (3.10), the difference is of order $1/\sqrt{T}$. It is seen that NTE anomaly is absent for quantum 1D Tonks gas as well. In other words, the quantization of classical model does not induce NTE for 1D pure hard rods.

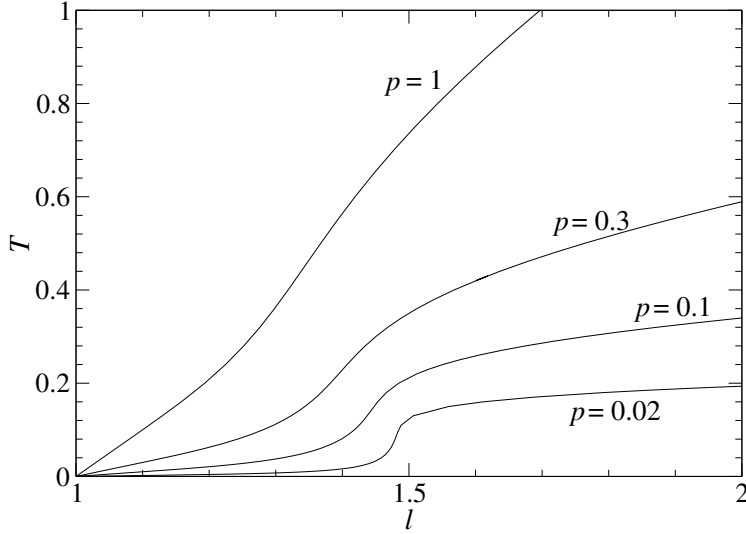


Fig. 3 SW model (4.1) with parameters $a = 1$, $a' = 2$ and $\varepsilon = 1$. The plot shows the dependence of T versus l for four values of the pressure $p = 1, 0.3, 0.1$ and 0.02 .

4 Square well model

The square well (SW) model is defined by the interaction potential (1.3) with [43]

$$\varphi(x) = -\varepsilon, \quad a < |x| < a' \quad (4.1)$$

where the well depth $\varepsilon > 0$. This soft-core potential is discontinuous at both $|x| = a$ and $|x| = a'$.

The Laplace transform (2.6) becomes [53]

$$\widehat{\Omega}(s) = \frac{e^{-a's} + e^{\beta\varepsilon}(e^{-as} - e^{-a's})}{s} \quad (4.2)$$

and the reciprocal density (2.8) reads as

$$l(T, p) = a' + \frac{T}{p} - \frac{a' - a}{1 - e^{-(a'-a)p/T} + e^{[-\varepsilon - (a'-a)p]/T}}. \quad (4.3)$$

The low-temperature dependence of EoS (4.3) is simple:

$$l = a + \frac{T}{p} + O(e^{-(a'-a)p/T}). \quad (4.4)$$

Thus for $T = 0$ the equidistant lattice spacing equals a , meaning any positive pressure pushes the particles to the hard core.

Let us choose the length parameters as follows $a = 1$, $a' = 2$ and the energy scale $\varepsilon = 1$, as shown by the dotted curve in figure 1. The plots of T versus l , given by (4.3), are shown in figure 3 for four values of the pressure

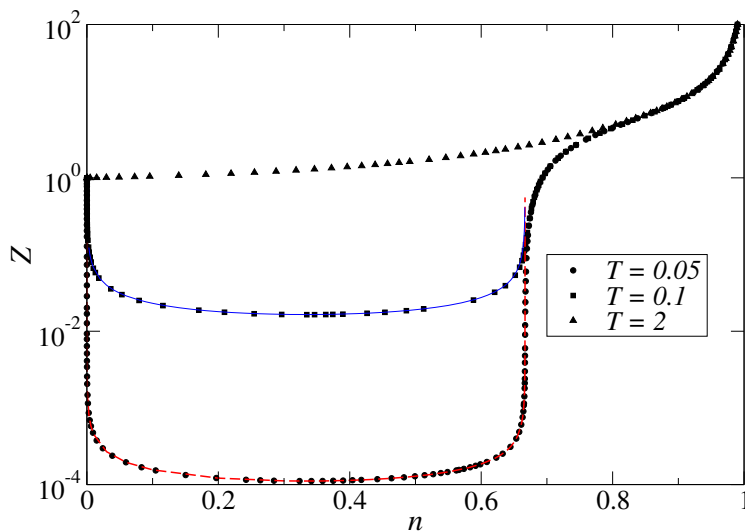


Fig. 4 SW model (4.1) with parameters $a = 1$, $a' = 2$ and $\varepsilon = 1$. The logarithmic plot of Z versus n is shown for three isotherms $T = 2$ (full triangles), $T = 0.1$ [full squares with solid-line prediction of (4.7)] and $T = 0.05$ [full circles with dashed-line prediction of (4.7)]. See the text for a detailed description of the plots.

$p = 1, 0.3, 0.1$ and 0.02 . Since l grows monotonously with T the anomalous NTE is absent for this model.

The compressibility factor Z is plotted as a function of the particle density n in figure 4 for three isotherms: $T = 2$ (full triangles), $T = 0.1$ (full squares) and $T = 0.05$ (full circles). The plot $Z(n)$ increases monotonously for the relatively large value of $T = 2$. For lower values of $T = 0.05$ and 0.1 , $Z(n)$ exhibits a steep descent in the region of very small n followed by a wide plateau inside which the pressure is very weak. The steep climb to values of order of unity takes place at around $n \approx 2/3$. $Z(n)$ exhibits the leading singularity of the expansion (2.31) when approaching $n \rightarrow 1^-$.

To derive a characteristic equation for the plateau region in the low- T regime, let us introduce the small variable

$$\lambda \equiv \exp(-\beta\varepsilon) \quad (4.5)$$

and make an analytic analysis of the EoS (4.3) in the regime $\lambda < \beta p(a' - a) < 1$. Equation (4.3) can be rewritten and treated as follows

$$\begin{aligned} Z &= a' \beta p + 1 - \frac{\beta p(a' - a)}{1 - e^{-\beta p(a' - a)}} \frac{1}{1 + \lambda \frac{1}{e^{\beta p(a' - a)} - 1}} \\ &\approx a' \beta p + 1 - \frac{1}{1 - \frac{1}{2} \beta p(a' - a)} \frac{1}{1 + \frac{\lambda}{\beta p(a' - a)}}, \end{aligned} \quad (4.6)$$

where the Taylor expansion of the exponentials in the last term on the rhs in powers of the small parameter $\beta p(a' - a)$ was used. Expanding once more the

rhs of (4.6) in small parameters $\beta p(a' - a)$ and $\lambda/[\beta p(a' - a)]$, and substituting $\beta p = Zn$, we end up with

$$Z \approx \sqrt{\frac{\lambda}{n(a' - a) \left[1 - \frac{a+a'}{2}n\right]}}. \quad (4.7)$$

The validity of the formula $Z < 1$ is equivalent to the inequality

$$\frac{1}{2}(a'^2 - a^2)n^2 - (a' - a)n + \lambda < 0 \quad (4.8)$$

which leads to the condition for the density interval

$$n(a' - a) \in \left(\lambda, \frac{2(a' - a)}{a' + a} - \lambda\right). \quad (4.9)$$

For our specific choice of $a = 1$ and $a' = 2$, the density border $2(a' - a)/(a' + a) = 2/3$ coincides with the point at which the isotherms $T = 0.1$ and $T = 0.05$ climb, as shown in figure 4. As is seen in the same figure, the prediction of formula (4.7) for temperatures $T = 0.05$ (dashed curve) and $T = 0.1$ (solid curve) is very accurate within the density interval $n \in (0, 2/3)$.

The (repulsive) square shoulder potential is derived from the (attractive) SW potential by substituting $\varepsilon \rightarrow -\varepsilon$ ($\varepsilon > 0$) in equation (4.1). Its exact EoS coincides with (4.3) under the same substitution $\varepsilon \rightarrow -\varepsilon$. Despite the formal similarity between the two potentials, their physics are fundamentally different. In a range of the pressures and low temperatures, the square shoulder potential exhibits the NTE anomaly [45]. The plots of the compressibility factor Z versus n also show distinct behaviors [45].

5 Polynomial potentials with just one minimum

Let us now study purely attractive soft-core potentials $\varphi(x) \leq 0$ that possess a polynomial form. The studied polynomials are of orders 2 and 3.

5.1 Quadratic model

Based on a standard 1D model of harmonically coupled oscillators, we consider a 1D fluid with the quadratic interaction potential [42]

$$\varphi(x) = \varepsilon \frac{(|x| - a_m)^2}{(a' - a_m)^2} - \varepsilon, \quad a < |x| < a'. \quad (5.1)$$

The potential $\varphi(x)$ has a minimum at $x = a_m$ with the value $\varphi(a_m) = -\varepsilon$. At the potential border $x = a'$, while the soft-core potential is continuous, $\varphi(a') = 0$, its first derivative $\varphi'(x)$ is not continuous. Note that if one chooses $a_m = (a + a')/2$ the potential vanishes at $x \rightarrow a^+$, $\varphi(x \rightarrow a^+) = 0$.

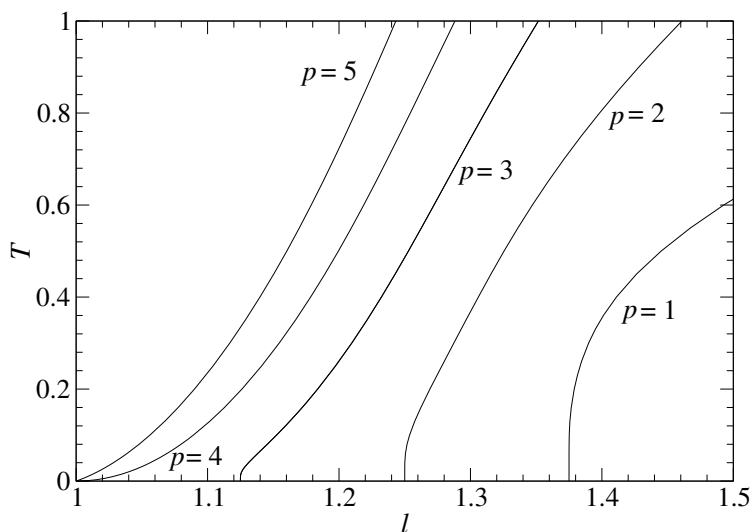


Fig. 5 Quadratic model with one minimum (5.1). Parameters are chosen as follows $a = 1$, $a_m = 3/2$, $a' = 2$, $\varepsilon = 1$ and the incompressibility pressure $p_i = 4$. The dependence of T versus l is plotted for five values of the pressure $p = 5, 4, 3, 2$ and 1 .

The Laplace transform (2.6) of the Boltzmann factor with the potential (5.1) takes the form

$$\hat{\Omega}(s) = \frac{e^{-a's}}{s} + \frac{\sqrt{\pi}}{2\sqrt{\beta\varepsilon}}(a' - a_m) \exp \left[\beta\varepsilon - a_m s + \frac{(a' - a_m)^2 s^2}{4\beta\varepsilon} \right] \times \left\{ \operatorname{erf} \left[\frac{2\beta\varepsilon + (a' - a_m)s}{2\sqrt{\beta\varepsilon}} \right] - \operatorname{erf} \left[\frac{2(a_m - a)\beta\varepsilon - (a' - a_m)^2 s}{2(a' - a_m)\sqrt{\beta\varepsilon}} \right] \right\}, \quad (5.2)$$

where

$$\operatorname{erf}(z) = \frac{2}{\sqrt{\pi}} \int_0^z dt e^{-t^2} \quad (5.3)$$

is the error function [54]. The rather complicated formula for the reciprocal density (2.8) is not presented here.

The ground-state spacing $l(T = 0, p)$ for pressures $0 < p < p_i$ can be deduced from (2.12),

$$l(T = 0, p) = x^*(p) = a_m - \frac{p(a' - a_m)^2}{2\varepsilon}, \quad \text{for } 0 < p < p_i. \quad (5.4)$$

The incompressibility pressure, given by the equality $l(T = 0, p_i) = a$, reads as

$$p_i = \frac{2\varepsilon(a_m - a)}{(a' - a_m)^2}. \quad (5.5)$$

The ground-state spacing remains equal to a for pressures larger than p_i ,

$$l(T = 0, p) = a, \quad \text{for } p \geq p_i. \quad (5.6)$$

The leading T -correction of the mean spacing $l(T, p)$ minus the ground-state spacing $l(T = 0, p)$ is given by

$$l(T, p) - l(0, p) = \begin{cases} \frac{T}{p - p_i} + O(T^2) & \text{if } p > p_i, \\ (a' - a_m)\sqrt{\frac{T}{\pi\varepsilon}} + \dots & \text{if } p = p_i, \\ \dots & \text{if } p < p_i. \end{cases} \quad (5.7)$$

The dots represent exponentially small terms of type $\exp(-c/T)$ with $c > 0$. The linear T -correction for $p > p_i$ coincides with that derived from (2.28) and the square-root \sqrt{T} -correction for $p = p_i$ coincides with that derived from (2.27). Since $\varphi''(x)$ does not depend on x , the derivative with respect to p on the rhs of (2.23) vanishes, signaling the absence of the term linear in T (and also higher powers of T) for $p < p_i$.

Choosing the parameters $a = 1$, $a_m = 3/2$, $a' = 2$ and $\varepsilon = 1$ in the definition of the quadratic potential (5.1), we find that the value of the potential at the minimum point $\varphi(3/2) = -1$, as shown by the dashed-dotted curve in figure 1. Formula (5.5) tells us that the incompressibility pressure $p_i = 4$. The dependence of T versus l is plotted for five values of the pressure $p = 5, 4, 3, 2$ and 1 in figure 5. It is evident that NTE is absent for this potential.

The isotherms of Z versus n are similar to those for the square well model in figure 4.

5.2 Cubic models

By fixing the parameters $a = 1$ and $a' = 2$, we introduce the cubic potential of the form

$$\varphi(x) = \alpha_1(x - 2) + \alpha_2(x - 2)^2 + \alpha_3(x - 2)^3 \quad (5.8)$$

ensuring the continuity of $\varphi(2) = 0$ at $x = 2$. Here, α_1 , α_2 and α_3 are real coefficient. Since

$$\varphi'''(x) = 6\alpha_3 \quad \text{for any } x \in [1, 2], \quad (5.9)$$

the sign of the coefficient α_3 determines the sign of the third derivative of $\varphi(x)$. We also require that $\varphi(1) = 0$, leading to the constraint

$$\alpha_2 = \alpha_1 + \alpha_3. \quad (5.10)$$

The condition for the minimum point a_m of the soft-core potential reads as

$$\left. \frac{\partial\varphi(x)}{\partial x} \right|_{x=a_m} = \alpha_1 + 2\alpha_2(a_m - 2) + 3\alpha_3(a_m - 2)^2 = 0. \quad (5.11)$$

The minimum point is expected to be within the interval $1 < a_m < 2$. It is useful to introduce new parameter t via

$$t \equiv 2 - a_m, \quad t \in (0, 1), \quad (5.12)$$

which represents the deviation of the minimum point a_m from the edge point 2. In terms of t equation (5.11) can be rewritten as

$$\alpha_1 - 2\alpha_2 t + 3\alpha_3 t^2 = 0. \quad (5.13)$$

The final requirement is that $\varphi(a_m) = -1$ which is equivalent to the relation

$$-\alpha_1 t + \alpha_2 t^2 - \alpha_3 t^3 = -1. \quad (5.14)$$

The three equations (5.10), (5.13) and (5.14) can be solved to express the coefficients α_1 , α_2 and α_3 in terms of t :

$$\alpha_1 = \frac{2 - 3t}{t(1-t)^2}, \quad \alpha_2 = \frac{1 - 3t^2}{t^2(1-t)^2}, \quad \alpha_3 = \frac{1 - 2t}{t^2(1-t)^2}. \quad (5.15)$$

Consequently,

$$\begin{aligned} t \in \left(0, \frac{1}{2}\right) &: \alpha_1, \alpha_2, \alpha_3 > 0, \\ t \in \left(\frac{1}{2}, \frac{1}{\sqrt{3}}\right) &: \alpha_1, \alpha_2 > 0, \quad \alpha_3 < 0, \\ t \in \left(\frac{1}{\sqrt{3}}, \frac{2}{3}\right) &: \alpha_1 > 0, \quad \alpha_2, \alpha_3 < 0, \\ t \in \left(\frac{2}{3}, 1\right) &: \alpha_1 \alpha_2, \alpha_3 < 0. \end{aligned} \quad (5.16)$$

The most significant change of sign is that of the coefficient α_3 which determines the sign of the third derivative of $\varphi(x)$ inside the whole region $x \in [1, 2]$, see equation (5.9). The positive values of α_3 correspond to the region of $t \in [0, 1/2]$, i.e., according to the relation (5.12), to the location of the minimum point on the right side from the interval center $3/2$, $a_m \in (3/2, 2)$. Such geometry of the interaction potential, depicted in figure 1 as ‘‘Cubic sharp to the right’’ of its minimum, forces particles to diminish their distance due to thermal fluctuations which indicates presence of NTE. On the other hand, the negative values of α_3 correspond to the region of $t \in [1/2, 1]$, meaning the minimum point is located to the left side of the interval center $3/2$, $a_m \in (1, 3/2)$. Such geometry of the interaction potential, depicted in figure 1 as ‘‘Cubic sharp to the left’’ of its minimum, forces particles to move further apart from each other due to thermal fluctuations, indicating absence of NTE.

Applying of the condition for the minimum point of the f -function (2.12) to the cubic potential (5.8) yields a second-degree equation for x^*

$$p + \alpha_1 + 2\alpha_2(x^* - 2) + 3\alpha_3(x^* - 2)^2 = 0. \quad (5.17)$$

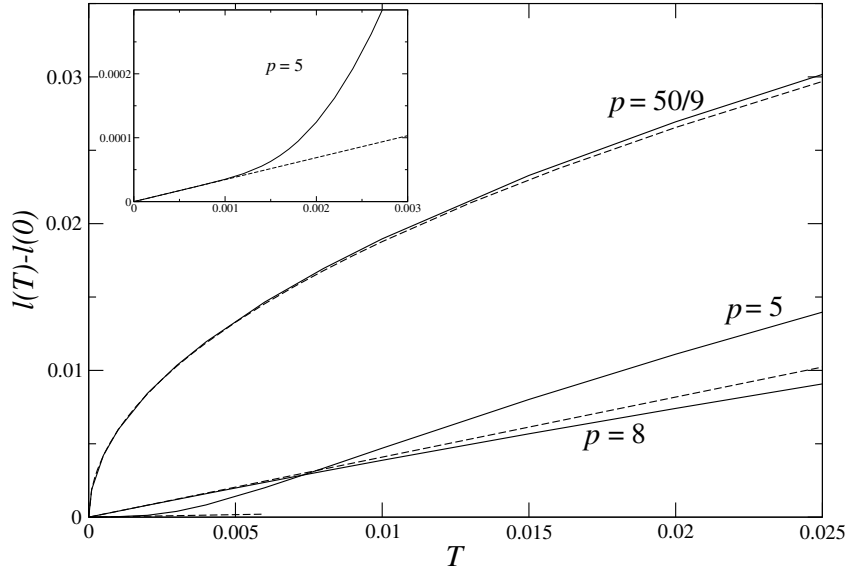


Fig. 6 Results for the cubic potential (5.19) with negative third derivative. The dependence of $l(T) - l(0)$ versus T is pictured for three values of the pressure $p = 8$, $p = p_c = 50/9 = 5.555\dots$ and $p = 5$ by solid curves. Dashed lines describe the plots given by the leading terms in (5.22). The inset magnifies the very-low-temperature region for $p = 5$.

The physically acceptable solution is

$$x^*(p, t) = \frac{1}{3(1-2t)} \left\{ 5 - 12t + 3t^2 + \sqrt{1 - 6t + 3(5-p)t^2 - 6(3-2p)t^3 + (9-15p)t^4 + 6pt^5} \right\}. \quad (5.18)$$

The plus sign ahead of the square root was chosen to ensure that for $p = 0$ (when $x^* = a_m$) it holds that $x^* = 2 - t$, in agreement with definition (5.12).

5.2.1 Cubic model with $\varphi'''(x) < 0$

Let us first consider negative coefficients α_3 , say the case $t = 3/5$ when

$$\varphi(x) = \frac{25}{36} [3(x-2) - 2(x-2)^2 - 5(x-2)^3]. \quad (5.19)$$

The minimum point of this potential occurs at $a_m = 7/5$ and $\varphi(a_m) = -1$ as it should be, see the dashed curve in figure 1. This cubic potential is sharp to the left of its minimum. It does not satisfy Kuzkin's condition (1.1) and therefore the absence of NTE anomaly is anticipated. A similar form and the absence of NTE is a common feature of many potentials, including the Lennard-Jones potential.

Integrals in the exact EoS (2.8) can only be treated numerically for the present potential. Nevertheless the ground state and leading terms of the low- T expansion of $l(T, p)$ can be found analytically. The substitution of $t = 3/5$ into equation (5.18) yields

$$x^*(p) = \frac{1}{75} \left(140 - \sqrt{5} \sqrt{245 + 108p} \right). \quad (5.20)$$

This $x^*(p)$ corresponds to the ground-state spacing between particles $l(T = 0, p)$ and varies continuously from the minimum point of the potential $a_m = 7/5$ when $p \rightarrow 0$ up to the smallest possible value $x = 1$ at the incompressibility pressure $p_i = 50/9$. In summary:

$$l(0, p) = \begin{cases} 1 & \text{if } p > p_i, \\ \frac{1}{75} \left(140 - \sqrt{5} \sqrt{245 + 108p} \right) & \text{if } 0 < p < p_i. \end{cases} \quad (5.21)$$

The coefficients of the leading low- T expansion of the difference $l(T, p) - l(0, p)$ can be obtained analytically from the previous formulas (2.23), (2.27) and (2.28):

$$l(T, p) - l(0, p) = \begin{cases} \frac{1}{6} T + O(T^2) & \text{if } p > p_i, \\ \frac{p - p_i}{5 \sqrt{13\pi}} \sqrt{T} + o(\sqrt{T}) & \text{if } p = p_i, \\ \frac{1}{245 + 108p} T + O(T^2) & \text{if } 0 < p < p_i. \end{cases} \quad (5.22)$$

Their check obtained by a numerical treatment of formula (2.8) is presented in figure 6 for three values of the pressure $p = 8$, $p = p_i = 50/9 = 5.555\dots$ and $p = 5$ (dashed lines) against the full values of the difference $l(T, p) - l(0, p)$ (solid lines). Since the leading T -term has an extremely small prefactor for $0 < p < p_i$, the inset magnifies the very-low-temperature region for $p = 5$.

The dependence of T versus l is plotted for five values of the pressure $p = 7, 6, 50/9, 3$ and 1 in figure 7. The plots do not exhibit the anomalous NTE behavior as was expected.

The isotherm curves of the dependences $Z(n)$ are similar to those of the SW model in figure 4.

5.2.2 Cubic model with $\varphi'''(x) > 0$

Now, let's consider positive coefficients α_3 , say the case $t = 1/3$ when

$$\varphi(x) = \frac{27}{4} [x - 2 + 2(x - 2)^2 + (x - 2)^3]. \quad (5.23)$$

The minimum point of this potential occurs at $a_m = 5/3$, see the solid curve in figure 1. This cubic potential is sharp to the right of its minimum and satisfies Kuzkin's condition (1.1), making it a candidate for NTE anomaly.

Substituting $t = 1/3$ into equation (5.18) results in

$$x^*(p) = \frac{1}{9} \left(12 + \sqrt{9 - 4p} \right). \quad (5.24)$$

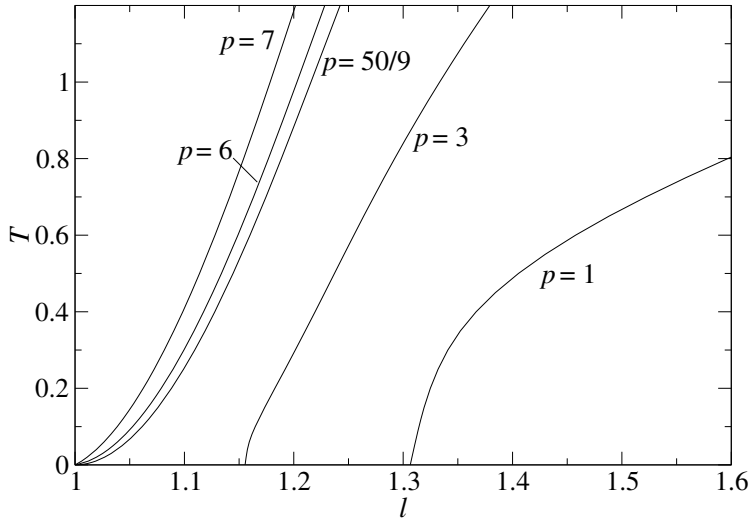


Fig. 7 Cubic model (5.19) with negative third derivative. The plot shows the relationship between T and l for five values of pressure $p = 7, 6, 50/9, 3$ and 1 . The value $50/9$ corresponds to the compressibility pressure p_i .

Similar to the previous case, this ground-state spacing between particles $l(0, p)$ moves continuously from the minimum point of the potential $a_m = 5/3$ as $p \rightarrow 0$. This continuous movement stops at specific “jump” pressure p_j before $x^*(p)$ reaches its smallest possible value 1 . This scenario is displayed in figure 8 where the plot of the function $f(x) = \varphi(x) + px$ (which needs to be minimized with respect to x in the interval $1 \leq x \leq 2$) is shown for three values of pressure: $p = 1.4$ (dash-dotted curve), $p = 27/16 = 1.6875 \dots$ (solid curve) and $p = 1.9$ (dashed curve). When $p = 1.4$ the only minimum point for $f(x)$ is given by (5.24). When the pressure reaches its jump value $p_j = 27/16$ the minimum of $f(x)$ is doubly degenerate at two points $x^*(p_j) = 3/2$ and $x = 1$. Increasing pressure beyond p_j , there is only one minimum of $f(x)$ at $x = 1$. Consequently, there is a jump between the minimums $x^*(p_j) = 3/2$ and $x = 1$ at $p = p_j$. The jump value of pressure $p_j = 27/16$ is determined by the relation

$$\varphi(x^*(p_j)) + p_j x^*(p_j) = \varphi(1) + p_j, \quad (5.25)$$

where

$$x^*(p_j) = \frac{1}{9} (12 + \sqrt{9 - 4p_j}). \quad (5.26)$$

To derive the value of the jump pressure for an arbitrary value of t , one inserts the expression (5.18) for the general $x^*(p, t)$ into equation (5.25), resulting in

$$p_j(t) = \frac{(2 - 3t)^2}{4(1 - t)^2(1 - 2t)}. \quad (5.27)$$

As a check we reproduce $p_j = 27/16$ for the above case $t = 1/3$. It is clear from figure 8 that the jump scenario occurs only if $f'(1) \geq 0$ at $p = p_j(t)$,

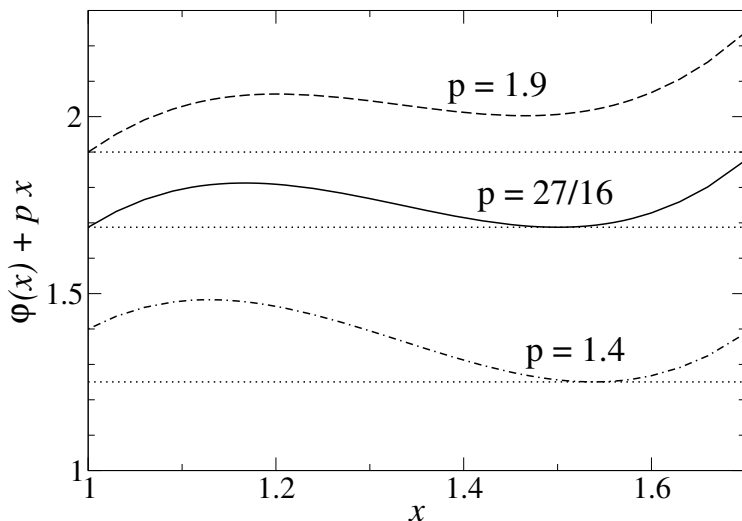


Fig. 8 The cubic model (5.23) with positive third derivative. The plot shows the function $f(x) = \varphi(x) + px$ for three pressure values: $p = 1.4$ (dash-dotted curve), $p = 27/16 = 1.6875\dots$ (solid curve) and $p = 1.9$ (dashed curve). Dotted lines indicate the minimum value of $f(x)$ for a given p on the interval $x \in [1, 2]$.

i.e.

$$p_j(t) \geq \frac{3t-1}{(1-t)t^2}. \quad (5.28)$$

By combining equations (5.27) and (5.28), we find that t must be from the interval $[0, 1/2)$, meaning the jump exists for all cubic potentials with positive third derivatives.

The formulas that include the ground state plus the leading low- T correction are written as

$$l(T, p) = \begin{cases} 1 + \frac{T}{p} + O(T^2) & \text{if } p > 27/16, \\ \frac{1}{9} \left(12 + \sqrt{9-4p} \right) - \frac{T}{9-4p} + O(T^2) & \text{if } 0 < p \leq 27/16. \end{cases} \quad (5.29)$$

For $0 < p \leq 27/16$, the prefactor $-1/(9-4p)$ to the linear- T term was derived from (2.23) and it was also checked numerically. It is important to note that this prefactor is negative throughout the interval $0 < p \leq 27/16$, providing a direct evidence of the NTE phenomenon. For $p > 27/16$, the prefactor $1/p$ to the linear- T term was obtained with a high precision numerically.

The plots of T versus l for six values of the pressure $p = 2, 1.8, 1.7, 27/16, 1$ and 0.5 are presented in figure 9. As is clear from equation (5.29), for $0 < p \leq p_j = 27/16 = 1.6875\dots$ the negative prefactor to the linear T -correction to $l(0)$ ensures the presence of NTE in the region of low temperatures, starting from $T = 0$. As documented in the figure on the case $p = 1.7$, NTE also remains in an interval of $p > p_j$, up to approximately $p \approx 1.75$, in spite of the positive prefactor $1/p$ to the linear T -correction to $l(0)$; NTE

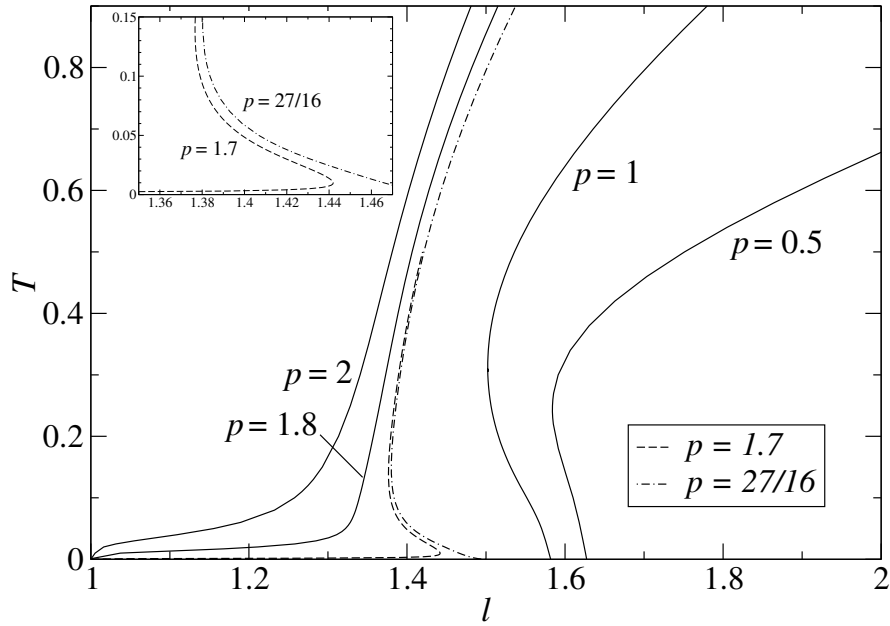


Fig. 9 Results for the cubic model (5.23) with positive third derivative. The dependence of T versus l for six distinct values of the pressure $p = 2, 1.8, 1.7, 27/16, 1$ and 0.5 . The inset magnifies the low-temperature region around $l \approx 1.4$ for two closely related pressure values $p_j = 27/16 = 1.6875 \dots$ (dash-dotted curve) and $p = 1.7$ (dashed curve). Refer to the text for a detailed description of the plots.

exists in an interval of low *strictly positive* temperatures excluding $T = 0$. The comparison of the curves for two close values of the pressure $p = 27/16 = 1.6875 \dots$ (dash-dotted curve) and $p = 1.7$ (dashed curve) in the inset of the figure indicates that NTE is related to the jump in $l(0)$ at p_j for $p \in [p_j, 1.75]$.

The dependence of Z versus n is plotted for three fixed values of the temperature $T = 1, 0.05$ and 0.02 in figure 10. For very low temperatures 0.02 and 0.05 , the plot $Z(n)$ exhibits two plateaus separated by a steep rise at $n \approx 1/a_m = 0.6$ and not very pronounced maximum and minimum around the higher plateau before transitioning into the asymptotic behavior $Z \approx 1/(1-n)$ in the limit $n \rightarrow 1^-$.

6 Models with non-analytic potentials

6.1 Fusion of two linear segments

The interaction potential of this model is defined by (1.3) with $\varphi(x)$ consisting of two linear segments connected at the minimum $x = a_m$ with $\varphi(a_m) = -\varepsilon$

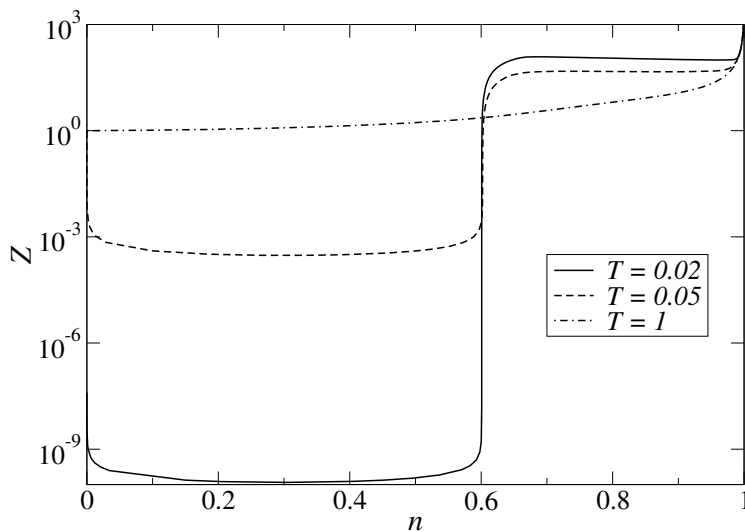


Fig. 10 Cubic model sharp to the right of its minimum (5.23). The dependence of Z versus n is plotted for three fixed values of the temperature $T = 1, 0.05$ and 0.02 .

($\varepsilon > 0$) and fulfilling the boundary conditions $\varphi(a) = \varepsilon_a$ and $\varphi(a') = 0$:

$$\varphi(x) = \begin{cases} -\frac{\varepsilon_a + \varepsilon}{a_m - a}|x| + \frac{a_m \varepsilon_a + a\varepsilon}{a_m - a} & \text{if } a < |x| < a_m, \\ \frac{\varepsilon}{a' - a_m}|x| - \frac{a'\varepsilon}{a' - a_m} & \text{if } a_m < |x| < a' \end{cases} \quad (6.1)$$

and $\varepsilon_a > -\varepsilon$. It is continuous for $|x| > a$, but its first derivative with respect to x is discontinuous, besides the border point $|x| = a'$, also at the minimum point $|x| = a_m$; denoting by a_n the position of the non-analyticity point one has $a_n = a_m$.

The Laplace transform (2.6) of the Boltzmann factor of the potential (6.1) and the reciprocal density (2.8) can be calculated analytically, but we do not present rather cumbersome formulas here. The incompressibility pressure $p_i = (\varepsilon + \varepsilon_a)/(a_m - a)$ is given by the slope of the first linear part of the interaction potential (6.1).

In the ground-state, the particle spacing behaves as

$$l(T = 0, p) = \begin{cases} a & \text{if } p > p_i, \\ \frac{a + a_m}{2} & \text{if } p = p_i, \\ a_m & \text{if } p < p_i. \end{cases} \quad (6.2)$$

This means that the particles form a close packed equidistant array with the hard-core spacing a for large pressures $p > p_i$. Below the transition pressure $0 < p < p_i$, the spacing becomes equal to a_m , i.e., the pressure is not able to kick a particle out of the potential minimum. The transition value $(a + a_m)/2$

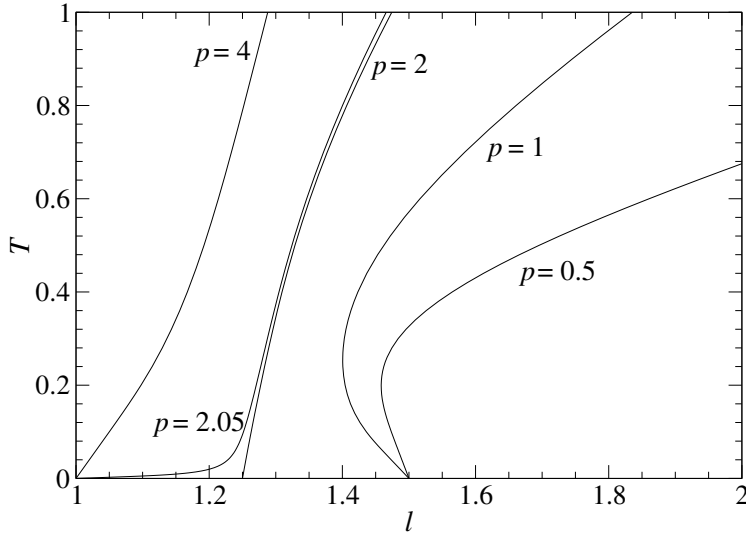


Fig. 11 The potential resulting from the fusion of two linear segments (6.1). Parameters are chosen as follows $a = 1$, $a_m = 3/2$, $a' = 2$, $\varepsilon = 1$, $\varepsilon_a = 0$ and the incompressible pressure $p_i = 2$. The dependence of T versus l is plotted for five fixed values of the pressure $p = 4, 2.05, 2, 1$ and 0.5 . Refer to the text for a detailed description of the plots.

at $p = p_i$ corresponds to a mixture of pair particle spacings a and a_m with the same density $1/2$. The ground-state prescription (2.12) cannot be applied to this model.

The leading temperature term is always linear in T , $l(T, p) - l(0, p) \sim \alpha(p)T$ in the limit $T \rightarrow 0^+$, where the prefactor α depends on the region of the pressure:

$$\alpha(p) = \begin{cases} 1 & \text{if } p > p_i, \\ \frac{p - p_i}{(a_m - a)(a' - a_m)} & \text{if } p = p_i, \\ \frac{2(a' - a_m)\varepsilon_a + (a' - a)\varepsilon}{(a' - a_m)(\varepsilon_a + \varepsilon) - (a_m - a)[\varepsilon + 2(a' - a_m)p]} & \text{if } p < p_i. \end{cases} \quad (6.3)$$

The prefactor is positive for $p > p_i$, diverging as p approaches the value p_i from above. It is finite and positive at $p = p_i$. The next correction terms are exponentially small, of type $\exp(-c/T)$ with $c > 0$, except for the transition pressure p_i when $l(T, p_i)$ exhibits Taylor's expansion in integer powers of T .

For the chosen parameters $a = 1$, $a_m = 3/2$, $a' = 2$, $\varepsilon_a = 0$ and $\varepsilon = 1$, the transition pressure is $p_i = 2$. The low- T expansion formula (6.3) now takes

the form

$$l(T, p) = \begin{cases} 1 + \frac{T}{p-2} + \dots & \text{if } p > 2, \\ \frac{5}{4} + \frac{T}{8} + O(T^2) & \text{if } p = 2, \\ \frac{3}{2} - \frac{p}{2[1-(p/2)^2]}T + \dots & \text{if } 0 < p < 2. \end{cases} \quad (6.4)$$

Note that the prefactor to T is negative if $0 < p < 2$ which is connected with existence of NTE in this interval of pressures. The plots of T versus l are shown for five fixed values of the pressure $p = 4, 2.05, 2, 1$ and 0.5 in figure 11. We can see NTE for $0 < p < 2$ as well as a jump of $l(0, p) \rightarrow 5/4$ at $p = p_i = 2$, see (6.4).

At low temperatures, the plot of $Z(n)$ shows two plateaus separated by a steep rise at $n \approx 1/a_m = 2/3$, similar to figure 10. This behavior is typical for models that exhibit a jump in $l(0, p)$.

6.2 Fusion of linear and quadratic models with non-analyticity point at $x = a_n < a_m$

Let's choose specific values for $a = 1$, $a_m = 3/2$, $a' = 2$ and the non-analyticity point connecting linear and quadratic parts of the interaction potential to the left of a_m , namely at $a_n = 5/4 = 1.25 < a_m$. Along with the conditions $\varphi(1) = \varphi(2) = 0$, we have

$$\varphi(x) = \begin{cases} 3 - 3x & \text{if } 1 < x < 5/4, \\ 4 \left(x - \frac{3}{2}\right)^2 - 1 & \text{if } 5/4 < x < 2. \end{cases} \quad (6.5)$$

Thus $\varphi(5/4) = -3/4$ is continuous, but its derivative $\varphi(x)'|_{x=5/4}$ is discontinuous. The Laplace transform (2.6) of the Boltzmann factor of the potential (6.5) reads as

$$\hat{\Omega}(s) = \frac{e^{-2s}}{s} + \frac{e^{(3\beta-5s)/4} - e^{-s}}{3\beta - s} + \frac{e^{\beta-3s/2+s^2/(16\beta)}\sqrt{\pi}}{4\sqrt{\beta}} \times \left\{ \operatorname{erf} \left[\frac{4\beta + s}{4\sqrt{\beta}} \right] - \operatorname{erf} \left[\frac{s - 2\beta}{4\sqrt{\beta}} \right] \right\} \quad (6.6)$$

which yields a lengthy explicit expression for $l(T, p)$ which is not presented here.

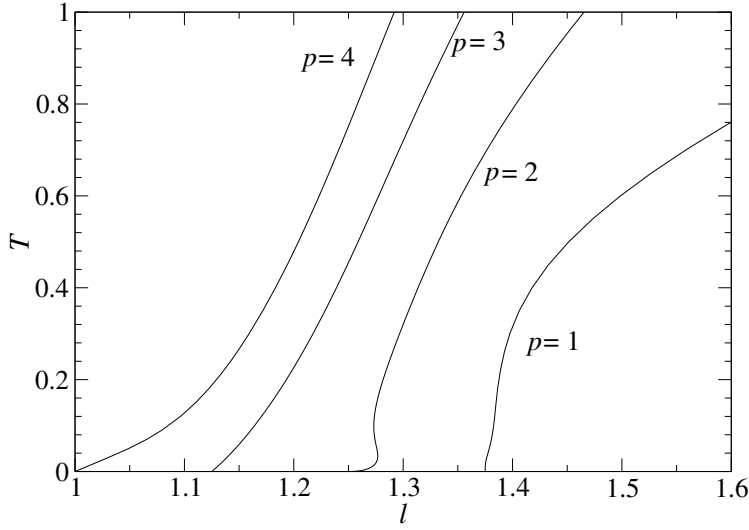


Fig. 12 Fusion of linear and quadratic models (6.5). The dependence of T versus l is plotted for four fixed values of the pressure $p = 4, 3, 2$ and 1 . The transition pressure $p_i = 3$ and NTE is seen at $p_n = 2$.

After some algebra the low- T expansion of $l(T, p)$ is found to be

$$l(p, T) = \begin{cases} 1 + \frac{T}{p-3} + O(T^2) & \text{if } p > 3, \\ \frac{9}{8} + \frac{T}{2} - 2T^2 + O(T^3) & \text{if } p = 3, \\ \frac{5}{4} + \frac{2(p-5/2)}{(p-2)(p-3)}T + O(T^2) & \text{if } 2 < p < 3, \\ \frac{5}{4} - \frac{4}{\sqrt{\pi}}T^{3/2} + O(T^2) & \text{if } p = 2, \\ \frac{3}{2} - \frac{p}{8} + \dots & \text{if } p < 2. \end{cases} \quad (6.7)$$

The dots mean an exponentially small term. There are two special pressures: $p_i = 3$ matches the slope of the linear part of $\varphi(x)$ and $p_n = 2$ is given by the non-analyticity point $x = 5/4$ which limits the validity of equation (2.12) to $l(0, p_n) = 3/2 - p_n/8 = 5/4$. The value $l(0) = 9/8 = (1 + 5/4)/2$ is the arithmetic mean at $p = p_i$. Note that the subleading terms tend to diverge when the pressure approaches special values, namely $p \rightarrow p_n^+$ and $p \rightarrow p_i$ from both sides.

The plots of $T(l)$ are shown in figure 12 for pressures $p = 1, p_n = 2, p_i = 3$ and $p = 4$. The NTE anomaly appears for medium pressures, for example, $p = 2$.

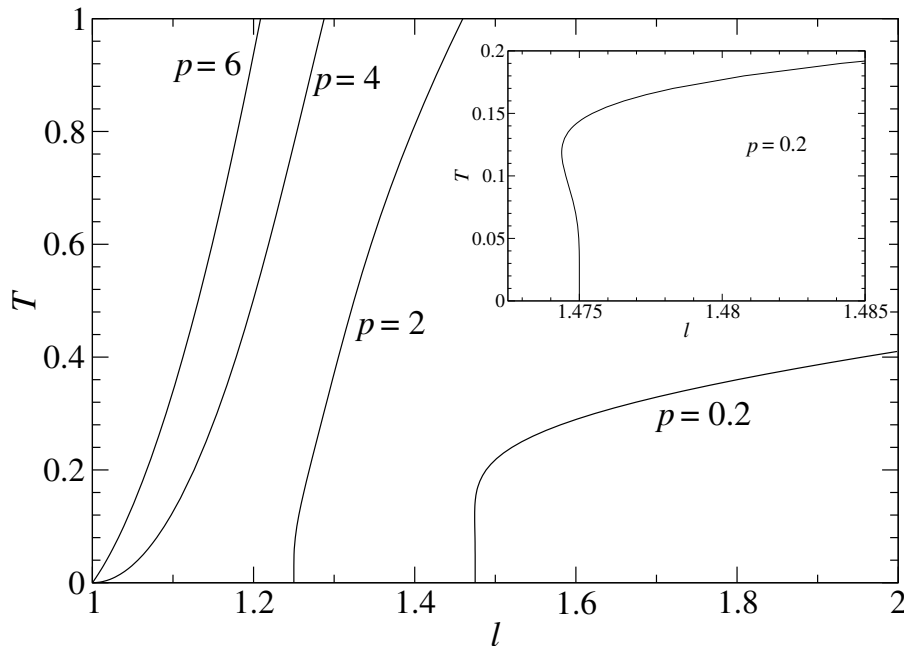


Fig. 13 Numerical results for the fusion model (6.8). The dependence of T versus l is shown for four different values of the pressure $p = 6, 4, 2$ and 0.2 . The inset magnifies the low-temperature region around $l(T = 0, p = 0.2)$ characterized by the presence of NTE.

6.3 Fusion of quadratic and linear models with non-analyticity point at $x = a_n > a_m$

We choose special values $a = 1$, $a_m = 3/2$, $a' = 2$ again and the non-analyticity point connecting linear and quadratic part of interaction at $a_n = 7/4 > a_m$. Together with the choice $\varphi(1) = \varphi(2) = 0$, the soft-core potential is given by

$$\varphi(x) = \begin{cases} 4 \left(x - \frac{3}{2} \right)^2 - 1 & \text{if } 1 < x < 7/4, \\ 3x - 6 & \text{if } 1 < x < 7/4. \end{cases} \quad (6.8)$$

Thus $\varphi(x)$ is continuous at $x = 7/4$, but its first derivative is discontinuous at this point.

The Laplace transform (2.6) of the Boltzmann factor of the potential (6.8) reads as

$$\hat{\Omega}(s) = \frac{e^{-2s}}{s} + \frac{e^{-2s} [e^{(3\beta+s)/4} - 1]}{3\beta + s} + \frac{e^{\beta-3s/2+s^2/(16\beta)} \sqrt{\pi}}{4\sqrt{\beta}} \times \left\{ \operatorname{erf} \left[\frac{4\beta - s}{4\sqrt{\beta}} \right] + \operatorname{erf} \left[\frac{2\beta + s}{4\sqrt{\beta}} \right] \right\}. \quad (6.9)$$

This equation provides the expression for $l(T, p)$ which is not included here. The ground state and low- T expansion of $l(T, p)$ can be written as

$$l(T, p) = \begin{cases} 1 + \frac{T}{p-4} - \frac{16 T^2}{(p-4)^3} + O(T^3) & \text{if } p > 4, \\ 1 + \frac{1}{2\sqrt{\pi}}\sqrt{T} + \dots & \text{if } p = 4, \\ \frac{3}{2} - \frac{p}{8} + \dots & \text{if } p < 4. \end{cases} \quad (6.10)$$

Here, the dots represent exponentially small terms. The incompressibility pressure $p_i = 4$ can be derived from (2.12) at the hard core $l(0, p_i) = 3/2 - p_i/8 = 1$.

In figure 13 we plot $T(l)$ for pressures $p = 0.2, 2, p_i = 4$ and $p = 6$. We still observe NTE for medium pressures, such as $p = 0.2$ but it is barely visible as shown in the inset.

7 Conclusion

Previous observations of the NTE anomaly in 2D and 3D systems of particles with anisotropic and isotropic pairwise interactions were limited to experiments and numerical simulations. Our previous work [45] on 1D hard rods with various types of soft repulsive nearest-neighbor interaction potentials allowed us to treat the NTE phenomenon based on exact thermodynamic results. The potentials have two competing length scales: the diameter of hard cores a (dominant at high temperatures and pressures) and the finite range a' of the soft component constrained by $a \leq a' \leq 2a$ (dominant at low temperatures and pressures). While we did not identify a precise mathematical criterion for the potential's characteristics that imply NTE, there are conditions that facilitate the emergence of NTE. One of these conditions is the jump in chain spacing $a' \rightarrow a$ of the equidistant ground state at certain pressures. Another condition is the non-analyticity of the soft potential $\varphi(x)$ within the interval $x \in (a, a')$. It is important to note that Kuzkin's necessary and sufficient condition for the presence of NTE (1.1) does not apply to these repulsive particle systems.

The present paper continues the discussion of NTE phenomenon in other exactly solvable 1D fluids.

First question studied in section 3 is whether the quantization of a classical fluid (which is free of NTE) can lead to NTE. To answer this question we use classical pure hard rods of diameter a which do not exhibit NTE and possess simple ground state: for an arbitrary pressure $p > 0$ the particle spacing equals to a , see section 3.1. As is shown in section 3.2, due to the uncertainty principle the quantum version of pure hard rods possesses a more complicated ground state with the particle spacing dependent on pressure p , see the relation (3.5). In spite of a shift of the ground-state spacing with respect to a for finite $p > 0$, the quantum curves of dependence T versus $l - a$ for fixed p (depicted in figure 2 by solid lines) are going to their classical counterparts (depicted in figure 2 by dashed lines) at infinite T monotonously. This

fact suggests an unimportant role of quantum mechanics in the generation of NTE in more general fluid models.

Secondly, the classical hard rods with various types of soft nearest-neighbor interactions that contain a basin of attraction with only one minimum are investigated. NTE occurs in two cases for such systems.

- As shown in section 5.2 for cubic potentials, NTE is present if Kuzkin’s condition (1.1) applies. It seems that in the derivation of Kuzkin’s condition the presence of an attractive basin for the potential is a necessary condition from the beginning. This also means that it is a sufficient condition but not a necessary one. The NTE phenomenon is accompanied by a jump in the equidistant ground state in spacing at a certain pressure p_j .
- As shown in section 6, NTE occurs as soon as the soft potential $\varphi(x)$ is non-analytic at a point within the interval $x \in (a, a')$. The position of the non-analyticity point a_n with respect to the minimum point of the potential a_m is irrelevant from this perspective, refer to section 6.1 for $a_n = a_m$, section 6.2 for $a_n < a_m$ and section 6.3 for $a_n > a_m$.

The compressibility factor $Z(\beta, n)$, introduced in section 2.3, is a thermodynamic quantity that exhibits a nontrivial behavior for our 1D fluids with nearest-neighbor interactions. In the case of purely repulsive interaction potentials [45], isotherms of Z as a function of the particle density n exhibit both monotonous and non-monotonous plots. In the present case of attractive interaction potentials, low-temperature isotherms of $Z(n)$ exhibit a steep descent for very small n , followed by a wide plateau up to $n \approx 2/3$ (for our choice of parameters) within which the pressure is very weak, as seen in figure 4 for the SW model. For the cubic model sharp to the right of its minimum, $Z(n)$ exhibits a double-plateau structure, as shown in figure 10.

The present treatment can be extended to mixtures, such as the polydisperse Tonks gas [43, 55].

It is known that degenerate Bose versions of 1D fluids can be prepared experimentally via a confinement in optical lattices [56, 57] and micro-traps [58, 59]. The Bethe-ansatz solution of the 1D Tonks gas [32, 33] can serve as a guide for an exact solution of a more general 1D quantum gas, for example, with square shoulder or well nearest-neighbor interactions.

Acknowledgements The support received from VEGA Grant No. 2/0089/24 is acknowledged.

Declarations

- Funding Not applicable
- Conflict of interest/Competing interests Not applicable
- Ethics approval and consent to participate Not applicable
- Consent for publication Not applicable
- Data availability Data are available upon a request.
- Materials availability Not applicable
- Code availability Not applicable

– Author contribution Not applicable

References

1. Röttger, K., Endriss, A., Ihringer, J., S. Doyle, S., Kuhs, W.F.: Lattice constants and thermal expansion of H₂O and D₂O ice Ih in between 10 and 265 K. *Acta Crystallogr. B* **50**, 644–648 (1994), <https://doi.org/10.1107/S0108768194004933>
2. Evans, J.S.O.: Negative thermal expansion materials. *J. Chem. Soc. Dalton Trans.* **19**, 3317–3326 (1999), <https://doi.org/10.1039/A904297K>
3. Greenwood, N.N., Earnshaw, A.: *Chemistry of the elements*, 2nd edn., Butterworth-Heinemann, (1997), <https://doi.org/10.1016/C2009-0-30414-6>.
4. Errington, J.R., Debenedetti, P.G.: Relationship between structural order and the anomalies of liquid water. *Nature (London)* **409**, 318–321 (2001), <https://doi.org/10.1038/35053024>
5. Yoon, D., Son, Y-W., Cheong, H.: Negative thermal expansion coefficient of graphene measured by Raman spectroscopy. *Nano Lett.* **11**, 3227–3231 (2011), <https://doi.org/10.1021/nl201488g>
6. Mary, T.A., Evans, J.S.O., Vogt, T., Sleight, A.W.: Negative thermal expansion from 0.3 to 1050 K in ZrW₂O₈. *Science* **272**, 90–92 (1996), <https://doi.org/10.1126/science.272.5258.90>
7. Biernacki, S., Scheffler, M.: Negative thermal expansion of diamond and zinc-blende semiconductors, *Phys. Rev. Lett.* **63**, 290–293 (1989), <https://doi.org/10.1103/PhysRevLett.63.290>
8. Forster, P.M., Yokochi, A., Sleight, A.W.: Enhanced negative thermal expansion in Lu₂W₃O₁₂. *J. Solid State Chem.* **140**, 157–158 (1998), <https://doi.org/10.1006/jssc.1998.7967>
9. Rechtsman, M.C., Stillinger, F.H., Torquato, S.: Negative thermal expansion in single-component systems with isotropic interactions. *J. Phys. Chem. A* **111**, 12816–12821 (2007), <https://doi.org/10.1021/jp076859l>
10. Kuzkin, V.A.: Comment on “Negative thermal expansion in single-component systems with isotropic interactions”. *J. Phys. Chem. A* **118**, 9793–9794 (2014), <https://doi.org/10.1021/jp509140n>
11. Batten, R.D., Stillinger, F.H., Torquato, S.: Novel low-temperature behavior in classical many-particle systems. *Phys. Rev. Lett.* **103**, 050602 (2009), <https://doi.org/10.1103/PhysRevLett.103.050602>
12. Batten, R.D., Stillinger, F.H., Torquato, S.: Interactions leading to disordered ground states and unusual low-temperature behavior. *Phys. Rev. E* **80**, 031105 (2009), <https://doi.org/10.1103/PhysRevE.80.031105>
13. Sadr-Lahijany, M.R., Scala, A., Buldyrev, S.V., Stanley, H.E.: Liquid-State anomalies and the Stell-Hemmer core-softened potential. *Phys. Rev. Lett.* **81**, 4895–4898 (1998), <https://doi.org/10.1103/PhysRevLett.81.4895>
14. Velasco, E., Mederos, L., Navascues, G., Hemmer, P.C., Stell, G.: Complex phase behavior induced by repulsive interactions. *Phys. Rev. Lett.* **85**, 122–125 (2000), <https://doi.org/10.1103/PhysRevLett.85.122>
15. Ryzhov, V.N., Stishov, S.M.: Repulsive step potential: A model for liquid-liquid phase transition. *Phys. Rev. E* **67**, 010201(R) (2003), <https://doi.org/10.1103/PhysRevE.67.010201>
16. Kumar, P., Buldyrev, S.V., Sciortino, F., Zaccarelli, E., Stanley, H.E.: Static and dynamic anomalies in a repulsive spherical ramp liquid: Theory and simulation. *Phys. Rev. E* **72**, 021501 (2005), <https://doi.org/10.1103/PhysRevE.72.021501>
17. Xu, L., Buldyrev, S.V., Angell, C.A., Stanley, H.E.: Thermodynamics and dynamics of the two-scale spherically symmetric Jagla ramp model of anomalous liquids. *Phys. Rev. E* **74**, 031108 (2006), <https://doi.org/10.1103/PhysRevE.74.031108>

18. Yan, Z., Buldyrev, S.V., Giovambattista, N., Debenedetti, P.G., Stanley, H.E.: Family of tunable spherically symmetric potentials that span the range from hard spheres to waterlike behavior. *Phys. Rev. E* **73**, 051204 (2006), <https://doi.org/10.1103/PhysRevE.73.051204>
19. Barros de Oliveira, A., Netz, P.A., Barbosa, M.C.: Which mechanism underlies the water-like anomalies in core-softened potentials?. *Eur. Phys. J. B* **64**, 481–486 (2008), <https://doi.org/10.1140/epjb/e2008-00101-6>
20. Barros de Oliveira, A., Netz, P.A., Barbosa, M.C.: An ubiquitous mechanism for water-like anomalies. *Europhys. Lett.* **85**, 36001 (2009), <https://doi.org/10.1209/0295-5075/85/36001>
21. Buldyrev, S.V., Malescio, G., Angell, C.A., Giovambattista, N., Prestipino, S., Saija, F., Stanley, H.E., Xu, L.: Unusual phase behavior of one-component systems with two-scale isotropic interactions. *J. Phys.: Condens. Matter* **21**, 504106 (2009), <https://doi.org/10.1088/0953-8984/21/50/504106>
22. Zhou, S., Solana, J.R.: Inquiry into thermodynamic behavior of hard spheres plus repulsive barrier of finite height. *J. Chem. Phys.* **131**, 204503 (2009), <https://doi.org/10.1063/1.3265984>
23. Coquand, O., Sperl, M.: Temperature expansions in the square shoulder fluid II: Thermodynamics. *J. Chem. Phys.* **152**, 124113 (2020), <https://doi.org/10.1063/1.5142662>
24. Hemmer, P.C., Stell, G.: Fluids with several phase transitions. *Phys. Rev. Lett.* **24**, 1284–1287 (1970), <https://doi.org/10.1103/PhysRevLett.24.1284>
25. Stell, G., Hemmer, P.C.: Phase transitions due to softness of the potential core. *J. Chem. Phys.* **56**, 4274–4286 (1972), <https://doi.org/10.1063/1.1677857>
26. Jagla, E.A.: Core-softened potentials and the anomalous properties of water. *J. Chem. Phys.* **111**, 8980–8986 (1999), <https://doi.org/10.1063/1.480241>
27. Fomin, Yu.D., Gribova, N.V., Ryzhov, V.N., Stishov, S.M., Frenkel, D.: Quasibinary amorphous phase in a three-dimensional system of particles with repulsive-shoulder interactions. *J. Chem. Phys.* **129**, 064512 (2008), <https://doi.org/10.1063/1.2965880>
28. Gribova, N.V., Fomin, Yu.D., Frenkel, D., Ryzhov, V.N.: Waterlike thermodynamic anomalies in a repulsive-shoulder potential system. *Phys. Rev. E* **79**, 051202 (2009), <https://doi.org/10.1103/PhysRevE.79.051202>
29. Stillinger, F.H., Stillinger, D.K.: Negative thermal expansion in the Gaussian core model. *Physica A* **244**, 358–369 (1997) [https://doi.org/10.1016/S0378-4371\(97\)00246-X](https://doi.org/10.1016/S0378-4371(97)00246-X)
30. Tonks, L.: The complete equation of state of one, two, and three dimensional gases of hard elastic spheres. *Phys. Rev.* **50**, 955–963 (1936), <https://doi.org/10.1103/PhysRev.50.955>
31. Zernike, F., Prins, J.A.: Die beugung von rontgenstrahlen in flussigkeiten als effekt der molekulanordnung. *Z. Physik* **41**, 184–194 (1927), <https://doi.org/10.1007/BF01391926>
32. Wadati, M., Kato, G.: One-dimensional hard-core Bose gas. *Chaos, Solitons & Fractals* **14**, 23–28 (2002), [https://doi.org/10.1016/S0960-0779\(01\)00178-3](https://doi.org/10.1016/S0960-0779(01)00178-3)
33. Šamaj, L., Bajnok, Z.: Introduction to the statistical physics of integrable many-body systems, Cambridge University Press, (2013), <https://doi.org/10.1017/CBO9781139343480>
34. Takahashi, H.: A simple method for treating the statistical mechanics of one-dimensional substances. *Proc. Phys. Math. Soc. Japan* **24**, 60–62 (1942), <https://doi.org/10.11429/ppmsj1919.24.0.60>
35. Bishop, M., Boonstra, M.: Exact partition functions for some one-dimensional models via the isobaric ensemble. *Am. J. Phys.* **51**, 564–566 (1983), <https://doi.org/10.1119/1.13204>
36. Salsburg, Z.W., Zwanzig, R.W., Kirkwood, J.G.: Molecular distribution functions in a one-dimensional fluid. *J. Chem. Phys.* **21**, 1098–1107 (1953), <https://doi.org/10.1063/1.1699116>
37. Lebowitz, J.L., Zomick, D.: Mixtures of hard spheres with nonadditive diameters: Some exact results and solution of PY equation. *J. Chem. Phys.* **54**, 3335–3346 (1971), <https://doi.org/10.1063/1.1675348>

-
38. Heying, M., Corti, D.S., The one-dimensional fully non-additive binary hard rod mixture: exact thermophysical properties. *Fluid Phase Equilib.* **220**, 85–103 (2004), <https://doi.org/10.1016/j.fluid.2004.02.018>
 39. Santos, A.: Exact bulk correlation functions in one-dimensional nonadditive hard-core mixtures. *Phys. Rev. E* **76**, 062201 (2007), <https://doi.org/10.1103/PhysRevE.76.062201>
 40. Ben-Naim, A., Santos, A.: Local and global properties of mixtures in one-dimensional systems, Part II: Exact results for the Kirkwood-Buff Integrals. *J. Chem. Phys.* **131**, 164512 (2009), <https://doi.org/10.1063/1.3256234>
 41. Sahnoun, A.Y., Djebbar, M., Benmessahib, T., Bakhti, B.: One dimensional lattice fluid mixture with nearest neighbour interactions. *J. Phys. A: Math. Theor.* **57**, 325007 (2024), [10.1088/1751-8121/ad6538](https://doi.org/10.1088/1751-8121/ad6538)
 42. Percus, J.K.: Exactly solvable models of classical many-body systems, In *Studies in Statistical Mechanics, vol. XIII Simple Models of Equilibrium and Nonequilibrium Phenomena* ed. J. L. Lebowitz, North Holland, (1987)
 43. Santos, A.: A Concise Course on the Theory of Classical Fluids, Chapter 5, Springer, (2016), <https://doi.org/10.1007/978-3-319-29668-5>
 44. Jones, G.L.: The low-temperature properties of the one-dimensional fluid. *J. Stat. Phys.* **44**, 237–248 (1985), <https://doi.org/10.1007/BF01010915>
 45. Travěnc, I., Šamaj, L.: 1D fluids with repulsive nearest-neighbour interactions: Low-temperature anomalies. *J. Phys. A: Math. Theor.* **58**, 195005 (2025), <https://doi.org/10.1088/1751-8121/add22c>
 46. Radin, C.: Low temperature and the origin of crystalline symmetry. *Int. J. Mod. Phys. B* **1**, 1157–1191 (1987), <https://doi.org/10.1142/S0217979287001675>
 47. Le Bris, C., Lions, P.-L.: From atoms to crystals: a mathematical journey. *Bull. Am. Math. Soc.* **42**, 291–363 (2005), <https://doi.org/10.1090/S0273-0979-05-01059-1>
 48. Blanc, X., Lewin, M.: The crystallization conjecture: a review. *EMS Surv. Math. Sci.* **2**, 255–306 (2015), <https://doi.org/10.4171/EMSS/13>
 49. Ventevögel, W.J.: On the configuration of a one-dimensional system of interacting particles with minimum potential energy per particle. *Physica A* **92**, 343–361 (1978), [https://doi.org/10.1016/0378-4371\(78\)90136-X](https://doi.org/10.1016/0378-4371(78)90136-X)
 50. Ventevögel, W.J., Nijboer, B.R.A.: On the configuration of systems of interacting particles with minimum potential energy per particle. *Physica A* **98**, 274–288 (1979), [https://doi.org/10.1016/0378-4371\(79\)90178-X](https://doi.org/10.1016/0378-4371(79)90178-X)
 51. Ventevögel, W.J., Nijboer, B.R.A.: On the configuration of systems of interacting particles with minimum potential energy per particle. *Physica A* **99**, 569–580 (1979), [https://doi.org/10.1016/0378-4371\(79\)90072-4](https://doi.org/10.1016/0378-4371(79)90072-4)
 52. Radin, C., Schulman, L.S.: Periodicity of classical ground states. *Phys. Rev. Lett.* **51**, 621–622 (1983), <https://doi.org/10.1103/PhysRevLett.51.621>
 53. Montero, A.M., Santos, A.: Triangle-Well and Ramp Interactions in One-Dimensional Fluids: A Fully Analytic Exact Solution. *J. Stat. Phys.* **175**, 269–288 (2019), <https://doi.org/10.1007/s10955-019-02255-x>
 54. Gradshteyn, I.S., Ryzhik, I.M.: *Table of Integrals, Series, and Products*, 6th edn., Academic Press, (2000), <https://doi.org/10.1090/s0025-5718-1972-0415970-6>
 55. Evans, M.R., Majumdar, S.N., Pagonabarraga, I., Trizac, E.: Condensation transition in polydisperse hard rods. *J. Chem. Phys.* **132**, 014102 (2010), <https://doi.org/10.1063/1.3263913>
 56. Kinoshita, T., Wenger, T., Weiss, D.S.: Observation of a one-dimensional Tonks-Girardeau gas. *Science* **305**, 1125–1128 (2004), <https://doi.org/10.1126/science.1100700>
 57. Haller, E., Hart, R., Mark, M.J., Danzl, J.G., Reichsollner, L., Gustavsson, M., Dalmon, M., Pupillo, G., Nagerl, H.-C.: Pinning quantum phase transition for a Luttinger liquid of strongly interacting bosons. *Nature* **466**, 597–600 (2010), <https://doi.org/10.1038/nature09259>
 58. Krüger, P., Hofferberth, S., Mazets, I.E., Lesanovsky, I., Schmiedmayer, J.: Weakly interacting Bose gas in the one-dimensional limit. *Phys. Rev. Lett.* **105**, 265302 (2010), <https://doi.org/10.1103/PhysRevLett.105.265302>
 59. Langen, T.: Non-equilibrium dynamics of one-dimensional Bose gases, Chapter 2, Springer, (2015), <https://doi.org/10.1007/978-3-319-18564-4>